THE UNIVERSITY OF READING

Grid Adaptation for 1-D Unsteady Problems

by

P. Garcia-Navarro

Numerical Analysis Report 9/95

DEPARTMENT OF MATHEMATICS

Grid adaptation for 1D unsteady problems

P. Garcia-Navarro

Abstract

One way to improve the results of the discretization of time-dependent partial differential equations is the redistribution of the grid according to the solution as it evolves. Three criteria are used to produce adapted grids in this report, and two different approaches are presented for the combining of the grid adaption and the solution of the differential equation. Only one dimensional scalar cases are considered.

1 Introduction

The work reported here was carried out with the purpose of obtaining a reliable grid adaptation method for unsteady problems involving sharp gradients. The aim of the work is the local refinement of a given grid by redistribution of the initial nodes according to a given criterion. Some work has been done in the past concerning re-gridding in steady problems or in unsteady problems tending to the steady state. The requirement of a grid adaptation in an advection problem, that is, to be a different shape every time step, imposes a new difficulty. In order to reduce the complexity of the calculation, only one-dimensional cases are considered and, to focus the attention on the basic ideas, the techniques are applied to scalar equations.

Two main types of grid adaptation algorithms can be distinguished depending on the use or not of a grid celerity in the process of resolution. The first group can be described as formed every time step by a sequence of

1. Updating the solution over Δt using a suitable numerical scheme.
2. Nodal displacement calculation according to a given criterion of equidistribution.
3. Grid updating
4. Redefinition of the solution on the new grid by means of a spatial interpolation.

This procedure has already proved to work well for applications involving the solution of time dependent equations for problems of evolution to the steady state. There are nevertheless doubts about, first, the convenience of using any interpolation, due to the risk of losing conservation, and second, the quality of the results obtained when using linear interpolation. The description interpolation methods will be used in what follows.

A second family of techniques is characterized by the explicit appearence of the grid celerity in the mathematical formulation. Interpolation is avoided by solving again on the unmodified grid with advection velocities corrected by the value of the grid celerity, that is, solving the problem relative to a grid which is not static. The basic algorithm every time step can be itemized as

1. Updating of the solution over Δt using a suitable numerical scheme giving predicted values.
2. Nodal displacement calculation according to a given criterion of equidistribution from the predicted values of the variable.
3. Grid celerity estimation $\dot{x}$
4. Recalculation of the solution over Δt using the celerity relative to the grid.
5. Grid updating.

These methods will be called *xdot* methods. The present report is concerned with the application and performance of the latter non interpolative procedure. There is freedom in the choice of the numerical scheme as well as in the node adaptation criterion. Several equidistribution algorithms will be presented. Explicit and implicit approaches will be implemented both for the numerical advection scheme and for the displacement calculation. The particular cases considered will be described and the results obtained will be shown and discussed in the next sections.

1.1 Test Problems

Two scalar equations have been chosen to test the performance of the grid adaptation techniques, the linear advection equation

$$\frac{\partial u}{\partial t} + a\frac{\partial u}{\partial x} = 0 \tag{1.1}$$

and the non linear Burgers' equation

$$\frac{\partial u}{\partial t} + u\frac{\partial u}{\partial x} = 0, \tag{1.2}$$

with the initial condition given by the curve

$$u(x) = u_m + u_d tanh(\alpha(x_c - x)) \tag{1.3}$$

$$u_m = 0.5(u_l + u_r)$$

$$u_d = 0.5(u_l - u_r)$$

where u_l and u_r are respectively the left and right values of the monoclinal curve. The value of α determines the steepness of the slope and x_c fixes the initial position of the point with ordinate u_m.

2 Grid adaptation criteria

Three criteria have been used to determine the grid movement. These are based on equidistribution of the function arclenght (EAL), the function first derivative (EF) and the function second derivative (E2D).

2.1 EAL distribution

With reference to Fig.1, given a grid $\{x_i, i = 1, imax\}$ and the discrete definition of a function $\{u_i\}$, two angles θ_R, θ_L can be associated to every internal node i, satisfying

$$cos\theta_L = \frac{x_i - x_{i-1}}{\Delta s_L} \quad , \quad cos\theta_R = \frac{x_{i+1} - x_i}{\Delta s_R}$$

where

$$\Delta s_L = \sqrt{(x_i - x_{i-1})^2 + (u_i - u_{i-1})^2}$$
$$\Delta s_R = \sqrt{(x_{i+1} - x_i)^2 + (u_{i+1} - u_i)^2}$$

are the left and right function arclength increments.
The equal arclength distribution can be stated as

$$\Delta s_L = \Delta s_R$$

for every internal node and can be rewritten

$$\frac{x_i - x_{i-1}}{cos\theta_L} = \frac{x_{i+1} - x_i}{cos\theta_R} \tag{2.1}$$

so that the following coupled system of equations results

$$A_i x_{i-1} + B_i x_i + C_i x_{i+1} = D_i.$$

The matrix of the system is tridiagonal and the system can be written

$$\begin{pmatrix} B_1 & C_1 & & & & \\ A_2 & B_2 & C_2 & & & \\ & A_3 & B_3 & C_3 & & \\ & & & \ddots & & \\ & & & A_{N-1} & B_{N-1} & C_{N-1} \\ & & & & A_N & B_N \end{pmatrix} \begin{pmatrix} X_1 \\ X_2 \\ X_3 \\ \vdots \\ X_{N-1} \\ X_N \end{pmatrix} = \begin{pmatrix} D_1 \\ 0 \\ 0 \\ \vdots \\ 0 \\ D_N \end{pmatrix} \tag{2.2}$$

The elements of the matrix are

$$A_i = -\frac{1}{cos\theta_L} \ , \ B_i = \frac{1}{cos\theta_L} + \frac{1}{cos\theta_R} \ , \ C_i = -\frac{1}{cos\theta_R}$$

for the interior points $\{i = 2, N-1\}$ whereas for the boundary points,

$$B_1 = 1 \ , \ C_1 = 0$$

$$A_N = 0 \ , \ B_N = 1,$$

D_1 and D_2 coming from the fixed positions of the extremes.

The system can be solved by means of a Thomas method for instance. An iterative procedure must be set up since the coefficients depend on the positions of the grid. Alternatively, rather than completely solve (2.2) and iterate on $cos\theta$, we can iterate for the solution of (2.2) (by, say, Jacobi's method), updating $cos\theta$ at each iteration. This is the procedure used in section 3 below. An example of the result after convergence to a fixed profile with $\alpha = 10$ is shown in Fig.2.

2.2 EF distribution

On the other hand, the equidistribution of the first derivative tends to concentrate grid points in the regions of strong gradient. It can be achieved starting from the previous description and imposing instead the equality of function increments on both sides of every internal node, i.e.

$$\Delta u_L = \Delta u_R$$

or

$$u_i - u_{i-1} = u_{i+1} - u_i.$$

We then have

$$\frac{(u_i - u_{i-1})}{(x_i - x_{i-1})}(x_i - x_{i-1}) = \frac{(u_{i+1} - u_i)}{(x_{i+1} - x_i)}(x_{i+1} - x_i), \tag{2.3}$$

which makes possible the construction of a new tridiagonal system

$$A_i x_{i-1} + B_i x_i + C_i x_{i+1} = D_i$$

where the coefficients are now

$$A_i = -tan\theta_L \quad , \quad B_i = tan\theta_L + tan\theta_R \quad , \quad C_i = -tan\theta_R$$

with

$$tan\theta_L = \frac{(u_i - u_{i-1})}{(x_i - x_{i-1})} \quad , \quad tan\theta_R = \frac{(u_{i+1} - u_i)}{(x_{i+1} - x_i)}$$

This criterion is less robust in the sense that it fails to converge when faced with steep gradients or very flat regions. The iterative solution of the system leads to a grid redistribution like the one plotted on Fig.3 for $\alpha = 5$.

2.3 E2D distribution

Now consider the third kind of equidistribution. There are several ways to formulate a grid adaptation based on the equidistribution of the second derivative. Some of them are presented here.

Along the lines of the two previous subsections, it can be required that

$$\Delta^2 u_L = \Delta^2 u_R$$

for every internal node. The next question is to decide the actual representation of $\Delta^2 u$. One possibility which presents itself is

$$\Delta^2 u_L = \frac{1}{2}(\Delta^2 u_i + \Delta^2 u_{i-1})$$

$$\Delta^2 u_R = \frac{1}{2}(\Delta^2 u_i + \Delta^2 u_{i+1}).$$

Then, using

$$\Delta^2 u_{i+1} = u_{i+2} - 2u_{i+1} + u_i = (u_{i+2} - u_{i+1}) - (u_{i+1} - u_i)$$

$$\Delta^2 u_{i-1} = u_i - 2u_{i-1} + u_{i-2} = (u_i - u_{i-1}) - (u_{i-1} - u_{i-2})$$

a pentadiagonal system of equations can be written whose typical equation is

$$A_i x_{i-2} + B_i x_{i-1} + C_i x_i + D_i x_{i+1} + E_i x_{i+2} = F_i$$

with

$$A_i = tan\theta_{LL}$$

$$B_i = -(tan\theta_{LL} + tan\theta_L)$$

$$C_i = tan\theta_R - tan\theta_L$$

$$D_i = -(tan\theta_R + tan\theta_{RR})$$

$$E_i = tan\theta_{RR}.$$

where

$$tan\theta_{LL} = \frac{(u_{i-1} - u_{i-2})}{(x_{i-1} - x_{i-2})} \quad , \quad tan\theta_{RR} = \frac{(u_{i+2} - u_{i+1})}{(x_{i+2} - x_{i+1})}.$$

The more complicated algebraic treatment required by the pentadiagonal system suggested seeking alternative formulations leading to tridiagonal systems.

With reference to Fig.1 again, it is possible to define a new weighting parameter related to the second derivative of the function as

$$w = \frac{\Delta x}{\Delta s'} = \frac{\Delta x}{\sqrt{(\Delta x)^2 + (\Delta u_x)^2}} = \frac{1}{\sqrt{(1 + (u_{xx})^2}}$$

The procedure used to enforce equal arc length distribution is repeated now. For every node the equidistribution

$$\Delta s'_L = \Delta s'_R$$

can be imposed, which can be rewritten

$$\frac{(x_i - x_{i-1})}{w_L} = \frac{(x_{i+1} - x_i)}{w_R},$$

so that it is possible to again have the system

$$A_i x_{i-1} + B_i x_i + C_i x_{i+1} = D_i$$

where the coefficients are

$$A_i = -\frac{1}{w_L} \quad , \quad B_i = \frac{1}{w_L} + \frac{1}{w_R} \quad , \quad C_i = -\frac{1}{w_R}.$$

Since w depends on the discrete second derivative, there is still some freedom in this choice. We have tried two approaches. The first one defines

$$(u_{xx})_L = \frac{\frac{1}{2}\left(\frac{(u_{i+1}-u_i)}{(x_{i+1}-x_i)} - \frac{(u_{i-1}-u_{i-2})}{(x_{i-1}-x_{i-2})}\right)}{x_i - x_{i-1}}$$

$$(u_{xx})_R = \frac{\frac{1}{2}\left(\frac{(u_{i+2}-u_{i+1})}{(x_{i+2}-x_{i+1})} - \frac{(u_i-u_{i-1})}{(x_i-x_{i-1})}\right)}{x_{i+1} - x_i} \tag{2.4}$$

Fig.4 shows the adaptation to a shape given by this criterion.

The second, taken from Blom et al., is

$$(u_{xx})_L = \frac{\frac{(u_{i+1}-u_{i-1})}{(x_{i+1}-x_{i-1})} - \frac{(u_i-u_{i-2})}{(x_i-x_{i-2})}}{x_i - x_{i-1}}$$

$$(u_{xx})_R = \frac{\frac{(u_{i+2}-u_i)}{(x_{i+2}-x_i)} - \frac{(u_{i+1}-u_{i-1})}{(x_{i+1}-x_{i-1})}}{x_{i+1} - x_i} \tag{2.5}$$

Fig.5 is the result of the adaptation based on this second approach.

Better solutions, in the sense of more flexible algorithms, are obtained by means of a combination of the arc length and second derivative weightings. In practice the weight

$$w_m = \frac{\Delta x}{\sqrt{(\Delta x)^2 + \beta_1(\Delta u)^2 + \beta_2(\Delta u_x)^2}}$$

has been used, whre β_1 and β_2 are parameters to be chosen. Figs. 6 and 7 result from this approach, with the discrete second derivative (2.4) and parameters $\beta_1 = 1, \beta_2 = 0.2$ and $\beta_1 = 0.2, \beta_2 = 1$, respectively.

Similarly, Figs. 8 and 9 are plots of the combinations $\beta_1 = 1, \beta_2 = 0.2$ and $\beta_1 = 0.2, \beta_2 = 1$ when using the discretization (2.5) for the term u_{xx}.

3 Explicit approach

We now combine the grid adaptation with the solution of the test equations. The updating numerical scheme used in this case was the first order upwind explicit scheme. For the nodal displacements, two criteria have been applied, the equidistribution of arclength (EAL) and the equidistribution of the first derivative of the variable (EF).

The celerity of the grid in this case has been explicitly defined from the value of the nodal displacement divided by the elapsed time. The value of every node displacement is explicitly calculated as

$$\Delta x_i = \frac{\Delta^2 s_i}{2(\frac{\Delta s_L}{\Delta x_L} + \frac{\Delta s_R}{\Delta x_R})}$$

in the case of equal arc length distribution, and as

$$\Delta x_i = \frac{\Delta^2 u_i}{2(tan\theta_R + tan\theta_L)}$$

in the case of equidistribution of the first derivative (see Baines). In the limit of iterations, i.e. after repeated use of these expressions to convergence, this two explicit expressions give the same result as the implicit equations previously presented in (2.1) and (2.3). The algorithm used is essentially the sequence suggested for the *xdot* methods in the Introduction.

A first result is presented corresponding to $x_c = L/2$, $\alpha = 10$, $u_l = 1$ and $u_r = -1$ in Burgers' equation. It is an example of pure compression and no advection. From the smooth initial curve, the solution steepens tending to a step like discontinuity between the left and right values in the initial position. Figs. 10 to 13 show the comparison of the results given by the interpolation and *xdot* methods using EAL and EF respectively.

The second test was made with the linear advection equation in order to explore the behaviour of the grid adaptation techniques in a pure advection situation. In this case, the numerical values are $x_c = L/4$, $\alpha = 10$, $u_l = 2$ and $u_r = 1$. Figs. 14 to 17 show the results. The curves in every plot represent the solution on the adaptive grid (moving) and the simply advected solution on a fixed grid (fixed).

A few tests were also done to show the convenience of iterating in the *xdot* method. The iteration involves repeating steps 2-4 in order to get a better fitting of the grid to the solution corresponding to the current time step. The results are not encouraging. Some of them are shown in Fig. 18 for the same test case as in Figs. 14-17. The equidistribution of arclength was carried out with iterations up to 20.

A third case is represented in Figs. 19 and 20. It is the nonlinear Burgers' equation with parameters $x_c = L/4$, $\alpha = 10$, $u_l = 2$ and $u_r = 1$. Comparison of the performances of the interpolation and the *xdot* methods can be seen on them.

The *xdot* methods seem to work better for pure compression problems, that is, for time dependent problems with no advection. In order to exploit the possible advantages offered by each technique, a special strategy was tested. It consists of solving a general advection equation in two steps, splitting the advection from the compression. For an equation like

$$\frac{\partial u}{\partial t} + \frac{\partial f}{\partial x} = 0 \tag{3.1}$$

which can be written

$$\frac{\partial u}{\partial t} + a\frac{\partial u}{\partial x} = 0 \tag{3.2}$$

with $a = f_u$ not constant in general, and initial conditions of the type (1.3) involving two states u_l and u_r, the following sequence is followed:

1. Definition of a constant average advection speed $\bar{a}$.

$$\bar{a} = \frac{f(L) - f(R)}{u(L) - u(R)} \tag{3.3}$$

2. Updating over one Δt of the linear advection equation

$$\frac{\partial u}{\partial t} + \bar{a}\frac{\partial u}{\partial x} = 0 \tag{3.4}$$

   by semi-lagrangian advection. In the first time step, it is possible to use the exact solution of (1.7). In the subsequent time steps, spatial interpolation is necesary. Linear interpolation and Euler time integration were used in the present report.

3. Application of the *xdot* method with equidistribution of the arclength to the equation

$$\frac{\partial u}{\partial t} + (a - \bar{a})\frac{\partial u}{\partial x} = 0. \tag{3.5}$$

Results of this approach are shown in Fig. 21. It shows the performance of the method for a slope $\alpha = 5$ of the initial profile. It is possible to introduce an iterative regridding step between 2 and 3 so that a better fitted grid is adapted to the advected solution is found before going to the *xdot* part. However, the method has turned out to be too diffusive as the plots make clear.

4 Implicit adaptation to advection

An implicit treatment of the problem can be made by coupling the implicit requirement of equidistribution of a property with an implicit discretization of the advection in a moving frame. This can be posed as the sequence

1. Adaptation of the grid to the initial conditions given a criterion of equidistribution using the implicit approach of section 2.
2. Updating of the solution over Δt using the celerity relative to the grid and a suitable implicit numerical scheme.
3. Implicit grid re-adaptation from the predicted values of the variable.

The advection part can be formulated as

$$\mathbf{M}(x^{n+1}, x^n, u^n)\mathbf{u}^{n+1} = \mathbf{r}$$

and the grid adaptation as

$$\mathbf{N}(u^{n+1}, x^n)\mathbf{x}^{n+1} = \mathbf{s}.$$

They are a pair of coupled systems of equations. Their solution can be achieved through an iterative process of repetition of steps 2-3 in which, at every time step, the solution from

$$\mathbf{M}[(x^{n+1})^p, x^n, u^n](\mathbf{u}^{n+1})^{p+1} = \mathbf{r} \tag{4.1}$$

is used to work out the coefficients of the system

$$\mathbf{N}[(u^{n+1})^p, x^n](\mathbf{x}^{n+1})^{p+1} = \mathbf{s} \tag{4.2}$$

and the solution to the latter used to improve the coefficients of the former until convergence is achieved.

Two points must be mentioned here. First, in order to start the iteration we shall need

$$p = 0 : (x^{n+1})^0 = x^n$$

where x^n stands for the best fitted grid to the initial conditions. Second, in order to find a converged solution the solutions to (4.1) and (4.2) are alternated, but seeking a convergence in the grid positions first. Then, convergence on the solution to the function is required on those grid positions. The grid convergence criterion is usually more relaxed than that for (4.1).

Results from this implicit version of the grid adaptation to a pure (linear) advection problem are presented in Figs. 22, 23 and 24. In all of them the advection with adaptation is compared both to the exact solution and to the numerical solution given by the advection on the initial fixed grid. Fig. 22 displays EAL distribution for a slope $\alpha = 10$ using $CFL = 1$ in this case. Fig. 23 contains results from EF distribution for a smoother profile ($\alpha = 5$) since convergence for steeper functions could not be achieved. Fig. 24 represents advection on a grid adapted according to the tridiagonal version of the 2nd derivative equidistribution using the first discretization and values $\beta_1 = 1, \beta_2 = 0.1$.

No results are presented from the application of the second type of E2D discretization since they were not good. Unlike in this study, Blom et al. use in their paper different strategies for the initial best grid adaptation and the subsequent redistributions. That might be another idea to try in future work.

As a last example, the adaptation to an unsteady nonlinear advection is displayed in Fig. 25. It corresponds to a test made with Burgers' equation and initial conditions

$$u_i = \begin{cases} u_L = 1 & \text{if } x_i \leq x_L = 0.5 \\ u_R = 0 & \text{if } x_i \geq x_R = 1.5 \\ ax_i + b & \text{otherwise} \end{cases}$$

The coefficients in the slope are

$$a = \frac{u_L - u_R}{x_L - x_R} \quad , \quad b = u_L - \frac{u_L - u_R}{x_L - x_R} x_L$$

The exact solution is a steepening of the slope in time until a sharp step shock is formed at t= $t_s = x_R - x_L$ in this case.

The results in Fig. 25 compare the solution on the EAL based adapted grid to the exact solution and to the one corresponding to a fixed grid.

5 Conclusions

The results of this study are not discouraging. The implicit treatment seems to be the one to follow for further work. Among the criteria tested to determine the regridding, the equal arc length distribution seems to be the more robust.
More work is necessary to get insight in the reasons for the weakness of the second derivative equidistribution in order to determine the correct treatment that would ensure convergence and avoid node overtaking.
Future work will be devoted to the extension to systems of equations in order to check the feasibility of this kind of approach when applied to practical advection problems.

6 Acknowledgment

The author wants to express her gratitude to Prof. Baines for his ideas and tutelage and also to Chris Smith and Matthew Hubbard for their time and interesting conversations.

References

[1] Baines M.J., *"Monotonic Adaptive Solutions of Transient Equations using Recovery, Fitting, Upwinding and Limiters."* Numerical Analysis Report, **5/92**, Department of Mathematics, University of Reading, 1992.

[2] Baines M.J., *"Properties of a Grid Movement Algorithm."* Numerical Analysis Report, **8/95**, Department of Mathematics, University of Reading, 1995.

[3] Blom J.G., Sanz-Serna J.M., Verwer J.G., *"On Simple Moving Grid Methods for 1D Evolutionary Partial Difference Equations."* Journal of Computational Physics, **74**, pp. 191-213, 1988.

[4] Bockelie M.J., Eiseman P.R., Smith R.E. *"A General Purpose Time Accurate Adaptive Grid Method."* 12th International Conference on Numerical Methods in Fluid Dynamics, Oxford, 1990.

[5] Dwyer H.A., *"Grid Adaption for Problems in Fluid Dynamics."* AIAA Journal, **22**, pp. 1705-1712, 1984.

[6] Hubbard M.E. and Baines M.J., *"Multidimensional Upwinding ad Grid Adaption."* In Numerical Methods for Fluid Dynamics V, Proceedings of the ICFD Conference Oxford, April 1995, Oxford University Press 1995.

[7] Smith C.J., *"Adaptive Finite Difference Solutions for Convection and Convection-Difussion Problems."* MSC Disertation, Department of Mathematics, University of Reading, 1992.

List of Figures

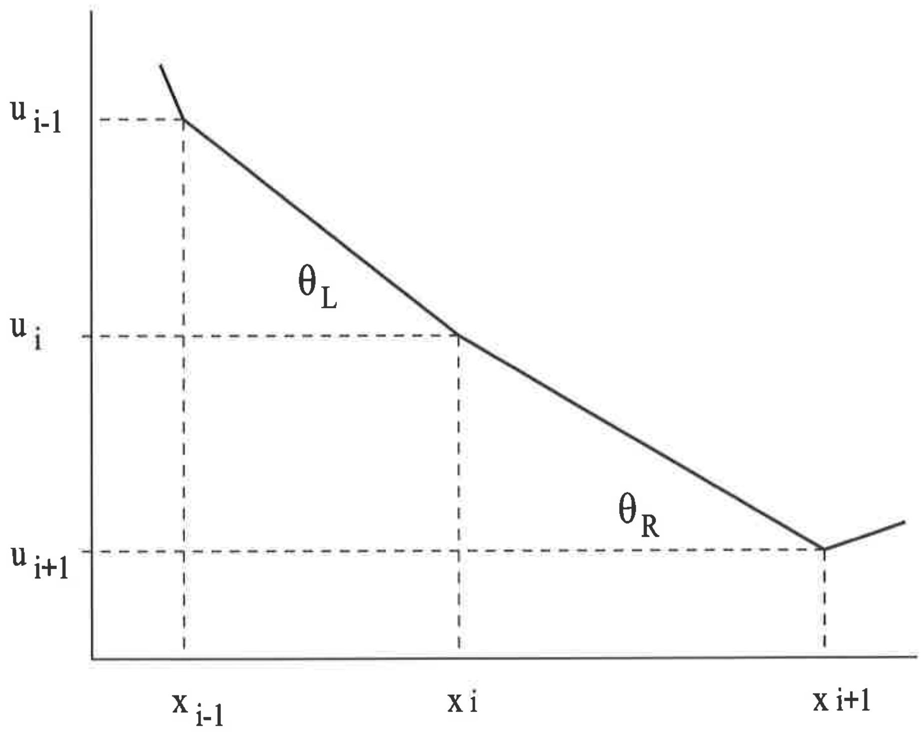

Figure 1: Discrete representation

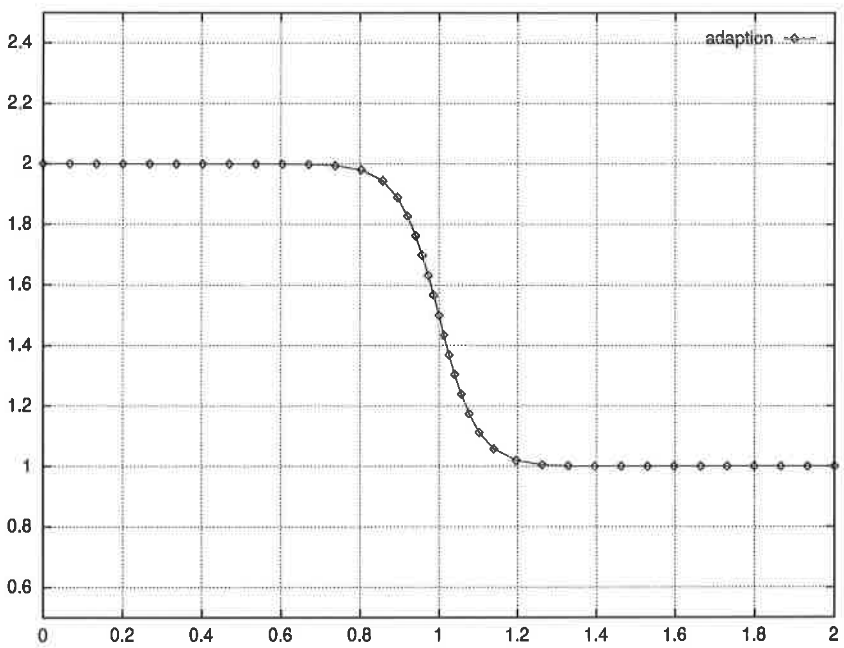

Figure 2: Equal arc length distribution. Fixed shape.

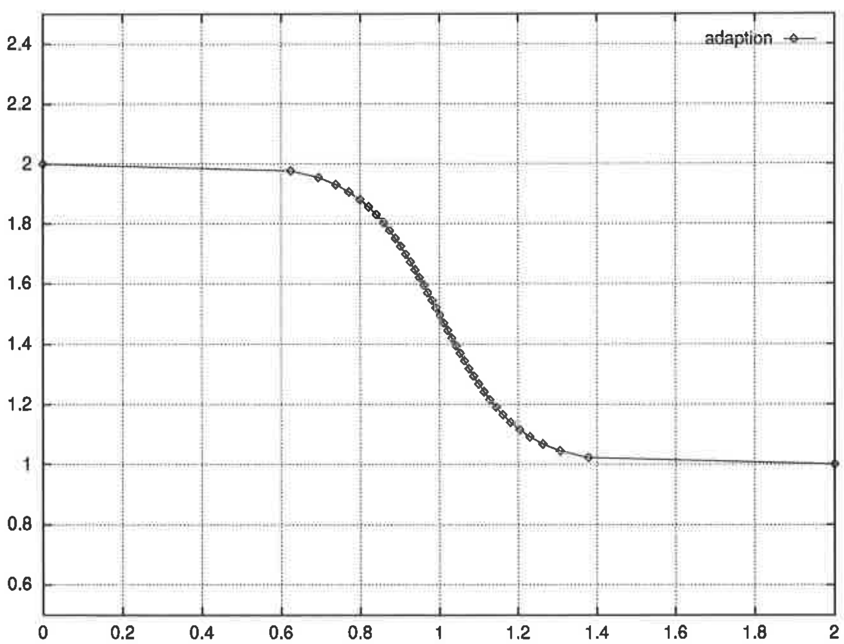

Figure 3: Equal first derivative distribution. Fixed shape.

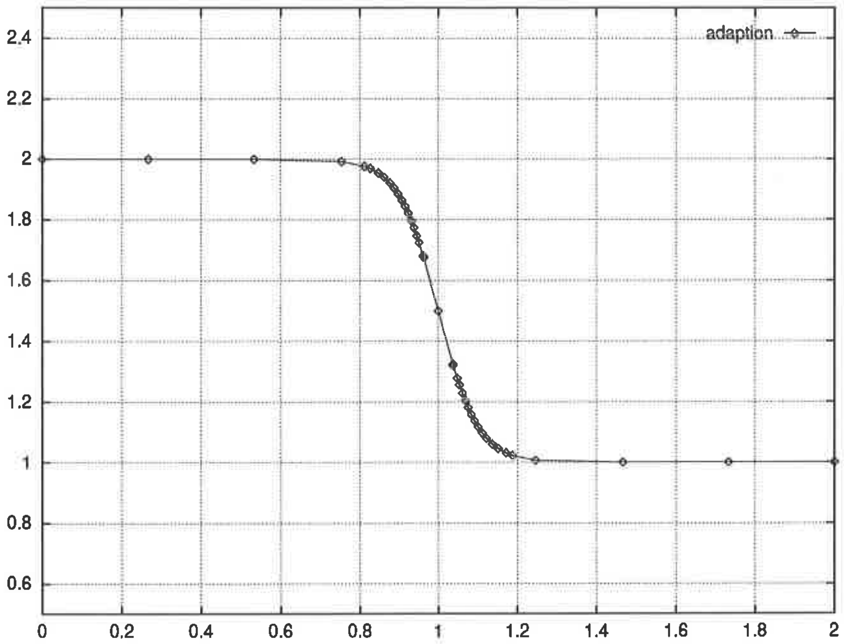

Figure 4: Equal second derivative distribution. First approach. Fixed shape.

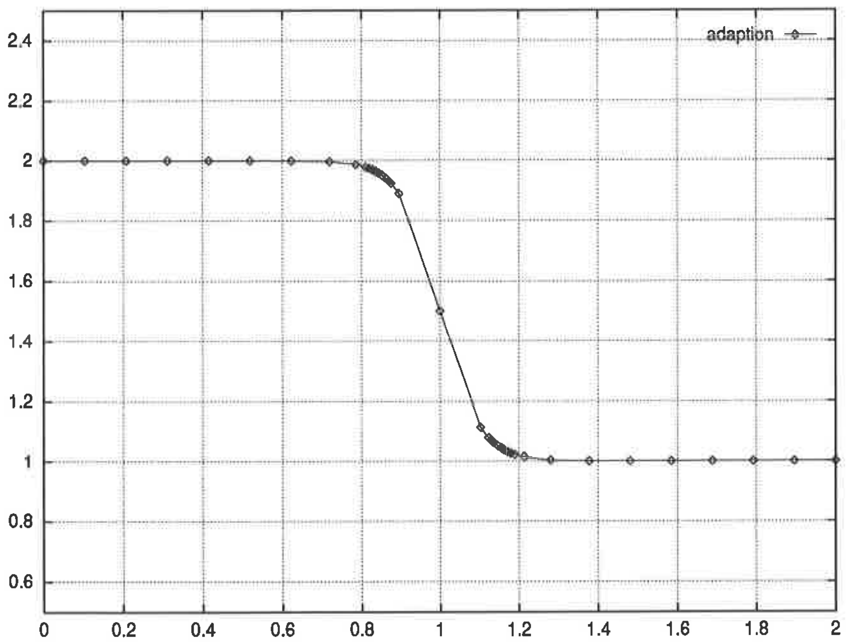

Figure 5: Equal second derivative distribution. Second approach. Fixed shape.

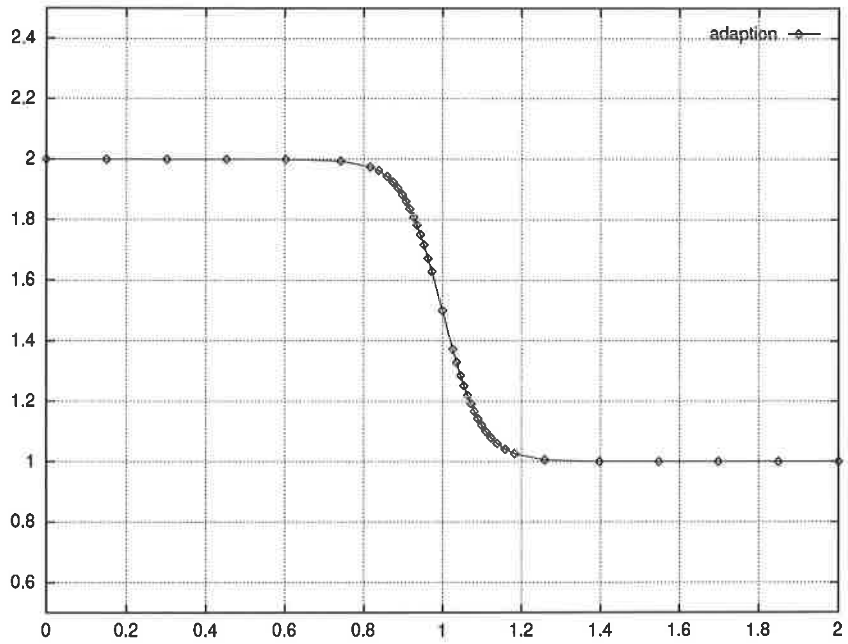

Figure 6: Equal second derivative distribution. First approach. $\beta_1 = 1, \beta_2 = 0.2$. Fixed shape.

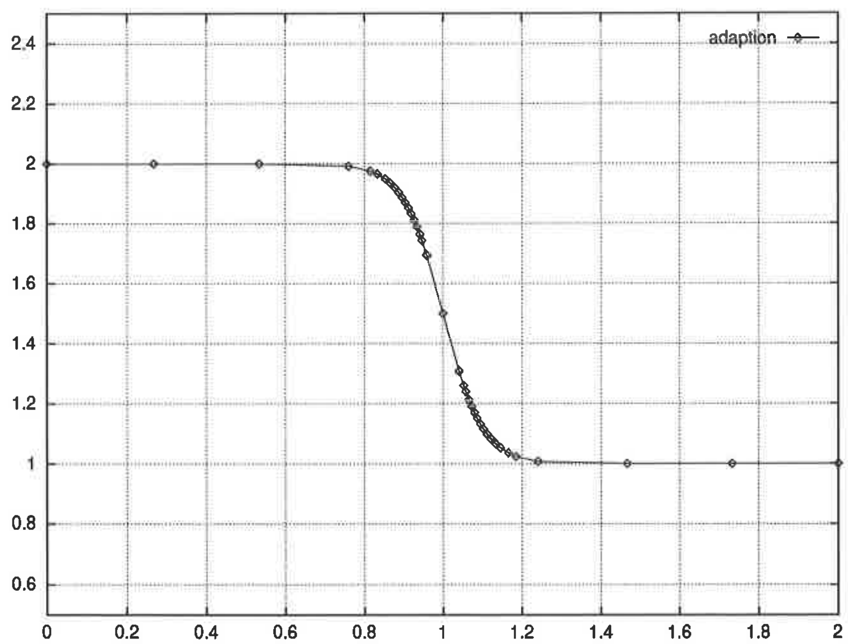

Figure 7: Equal second derivative distribution. Second approach. $\beta_1 = 0.2, \beta_2 = 1$. Fixed shape.

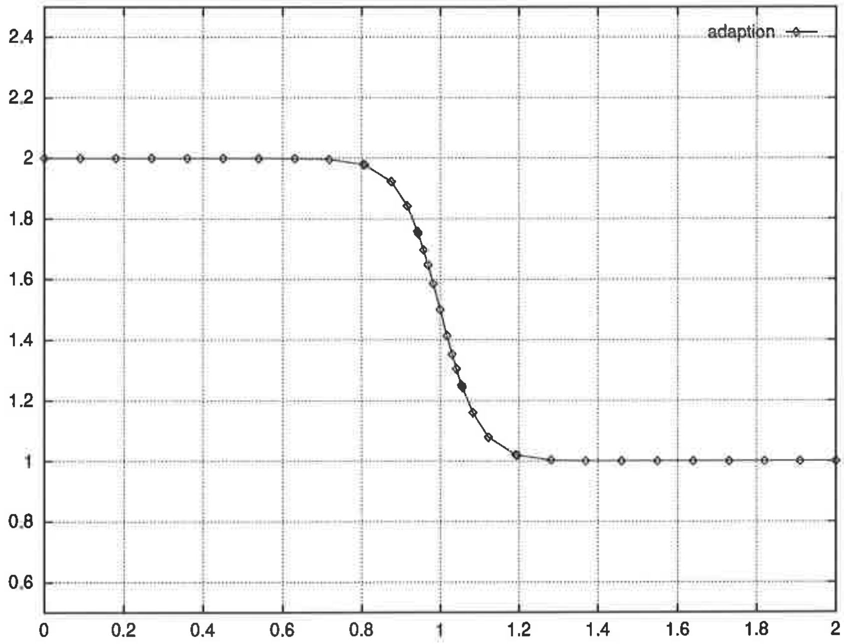

Figure 8: Equal second derivative distribution. First approach. $\beta_1 = 1, \beta_2 = 0.2$. Fixed shape.

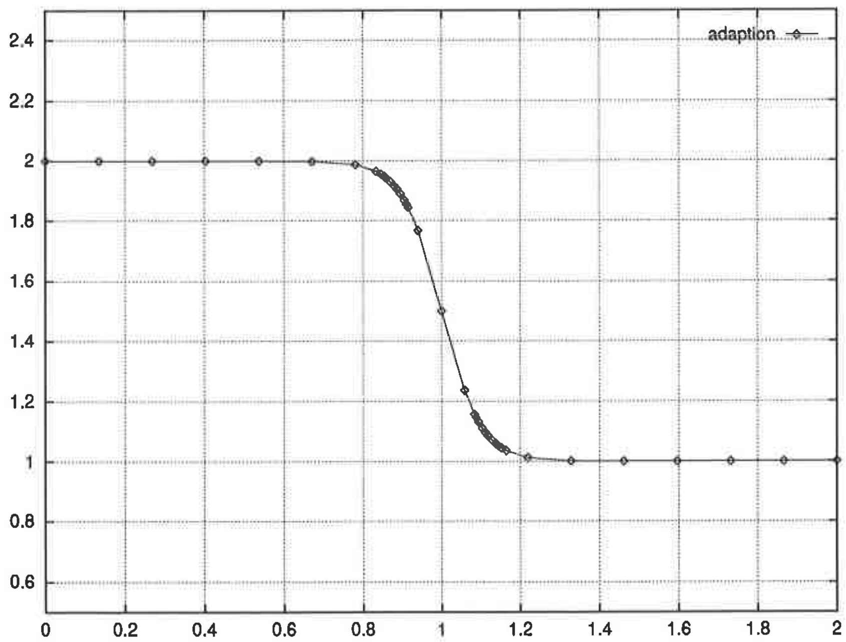

Figure 9: Equal second derivative distribution. Second approach. $\beta_1 = 0.2, \beta_2 = 1$. Fixed shape.

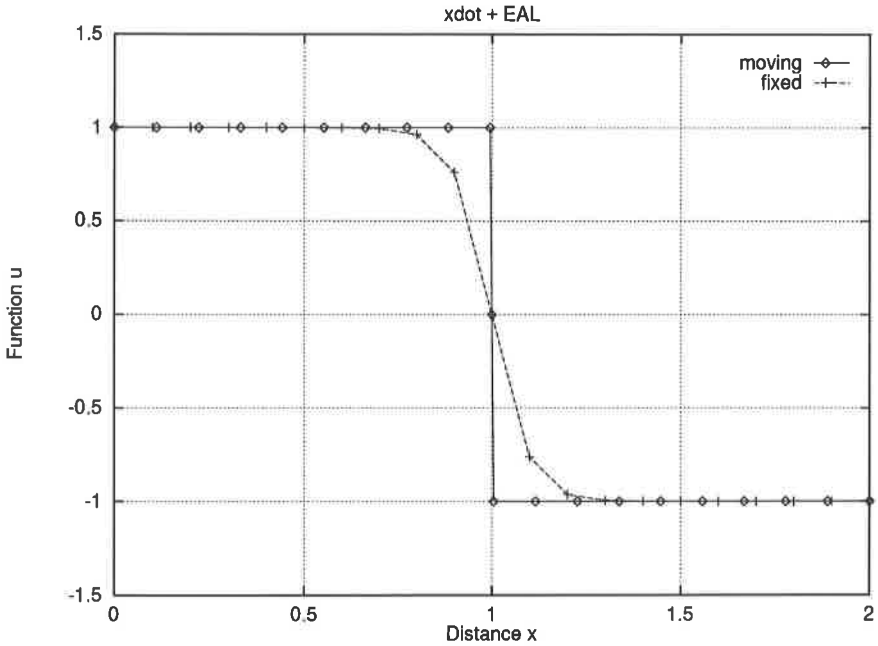

Figure 10: Equal arc length distribution. Explicit *xdot*. Pure compression.

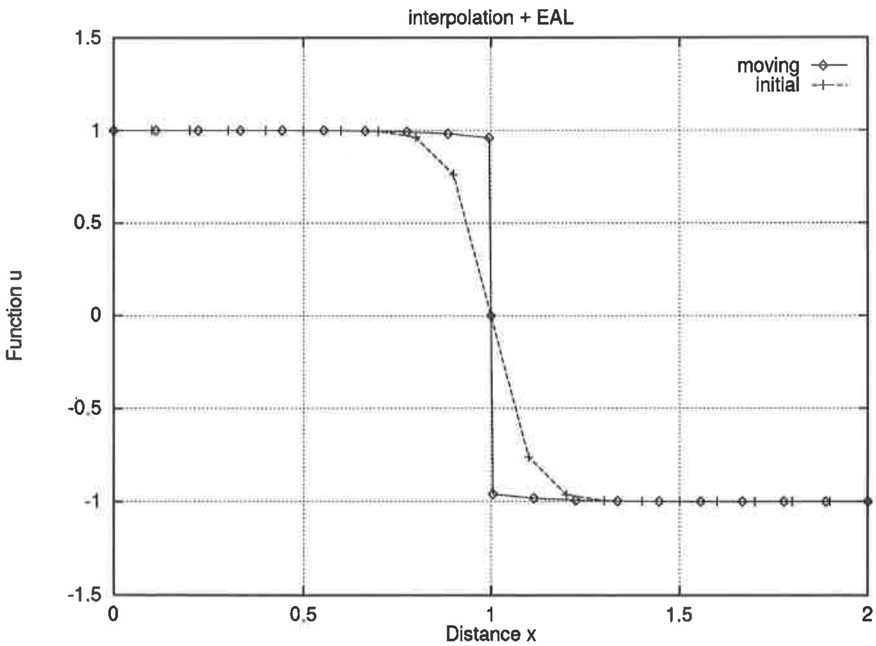

Figure 11: Equal arc length distribution. Interpolation. Pure compression.

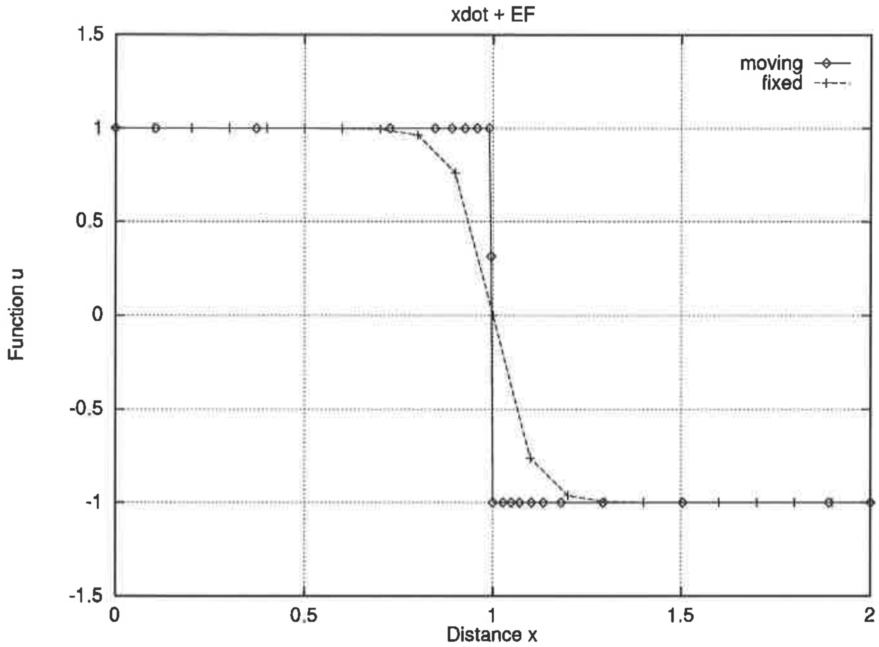

Figure 12: Equal arc length distribution. Explicit *xdot*. Pure compression.

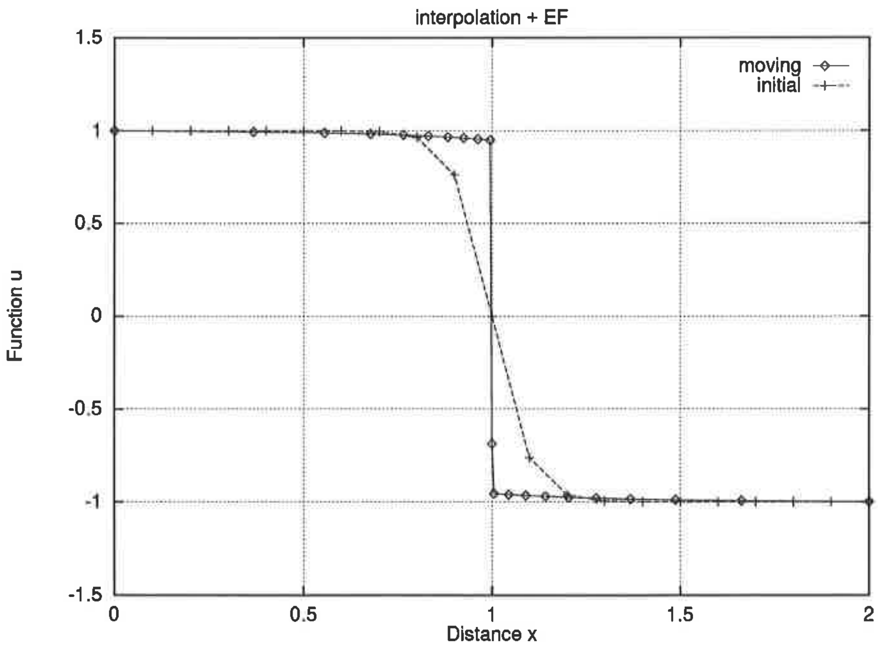

Figure 13: Equal arc length distribution. Interpolation. Pure compression.

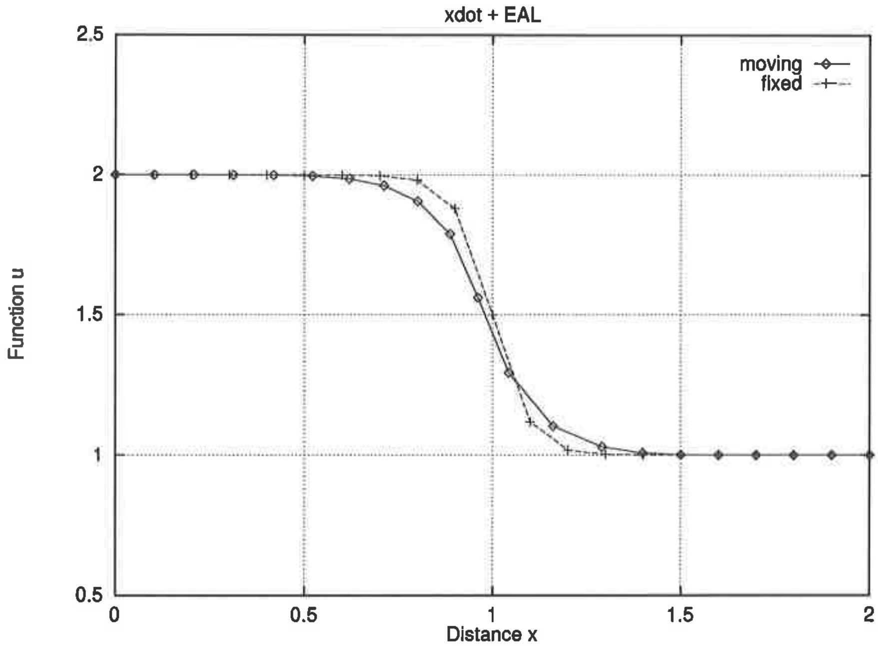

Figure 14: Equal arc length distribution. Explicit *xdot*. Linear advection.

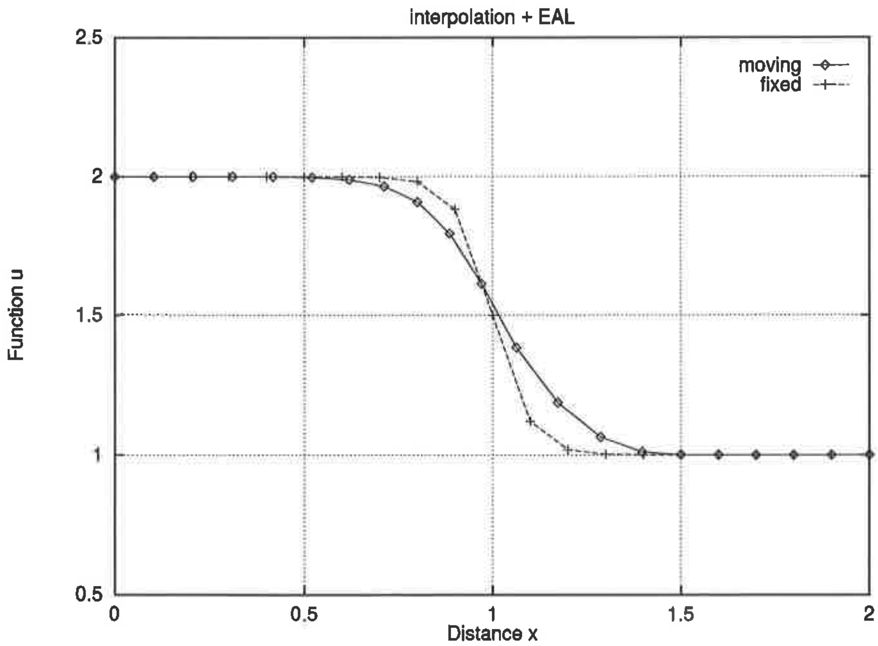

Figure 15: Equal arc length distribution. Interpolation. Linear advection.

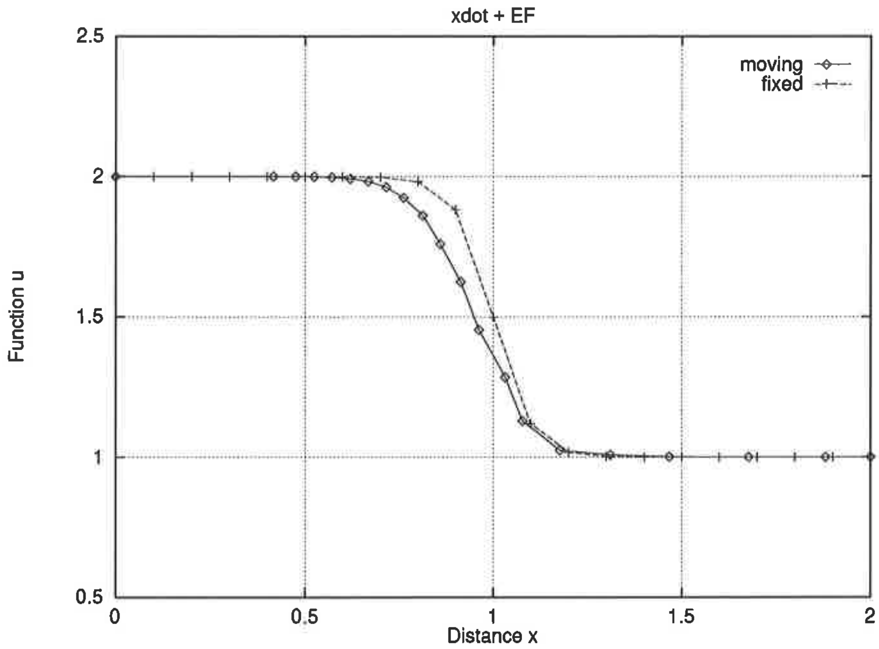

Figure 16: Equal 1st derivative distribution. Explicit *xdot*. Linear advection.

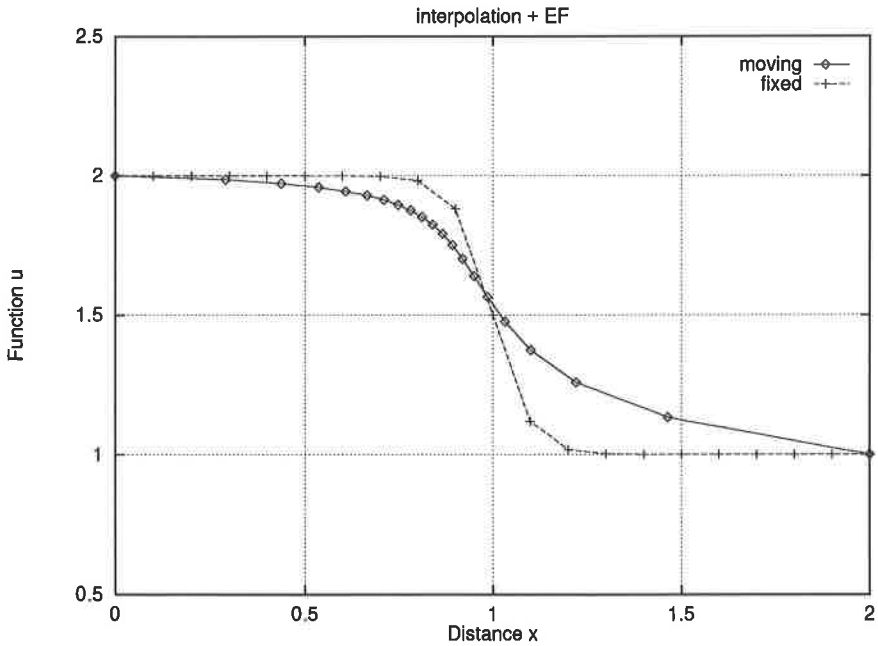

Figure 17: Equal 1st derivative distribution. Interpolation. Linear advection.

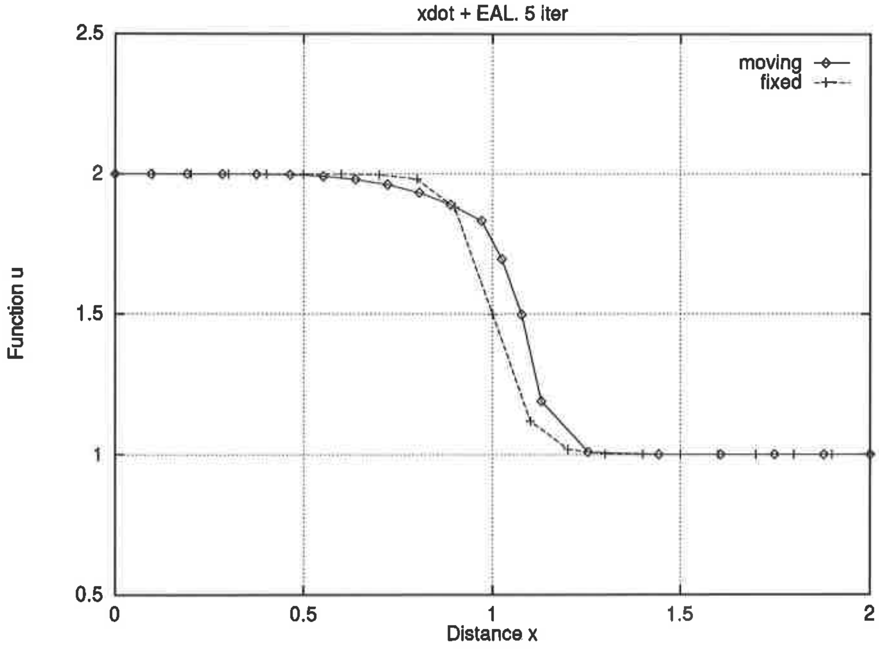

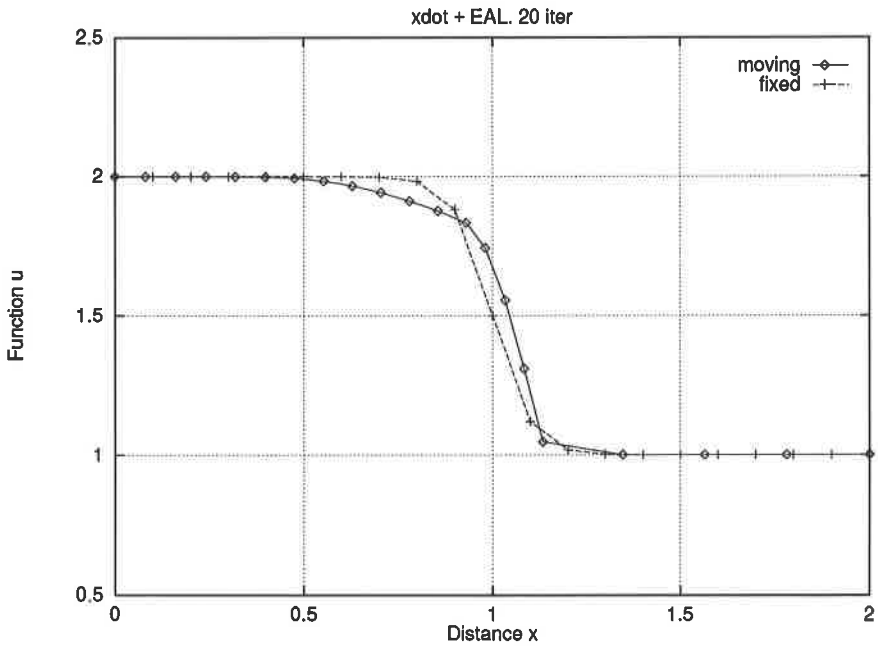

Figure 18: Equal arc length distribution with iterations. Upper 5 iterations. Lower 20 iterations. Linear advection

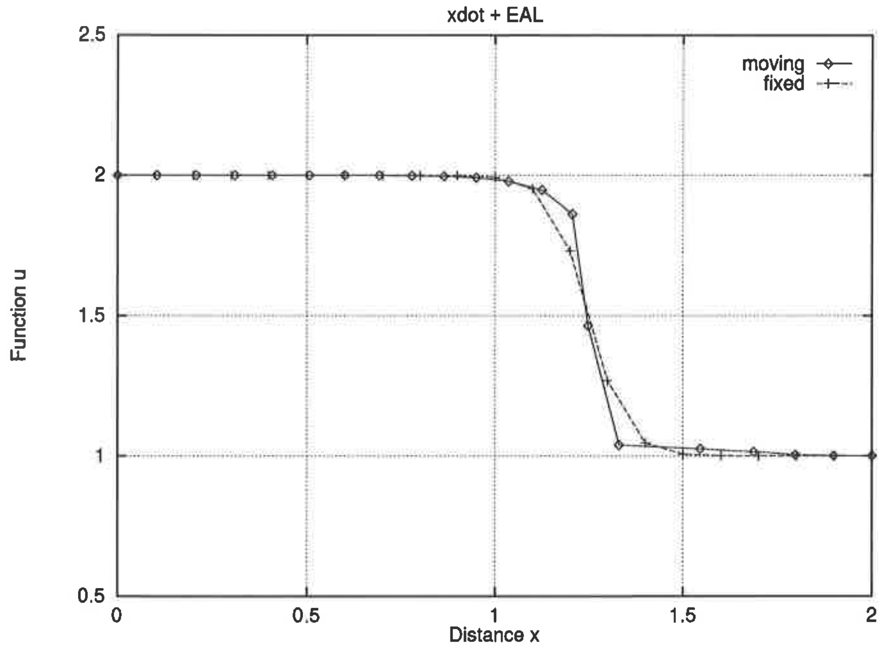

Figure 19: Equal arc length distribution. Explicit *xdot*. Nonlinear advection.

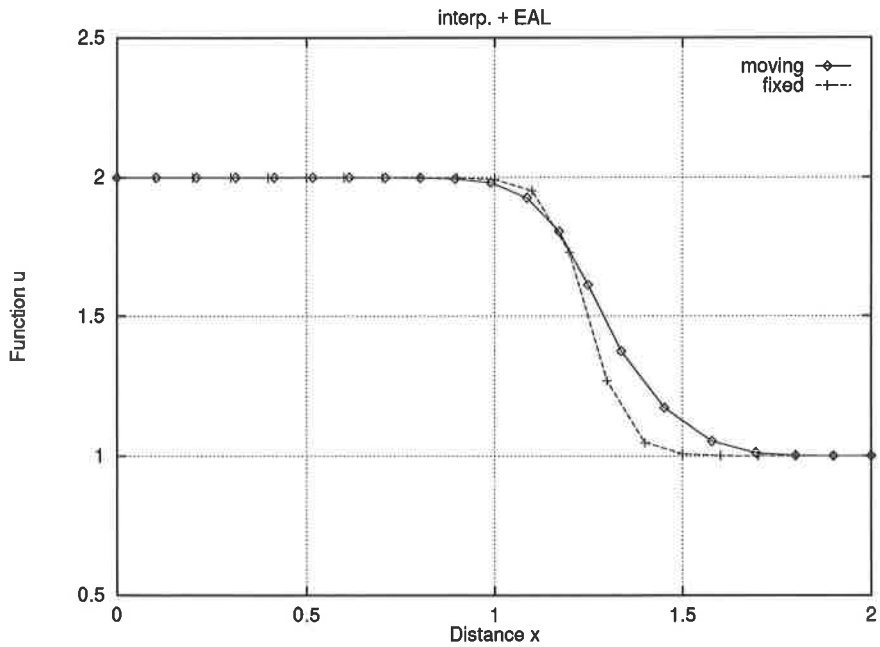

Figure 20: Equal arc length distribution. Interpolation. Nonlinear advection.

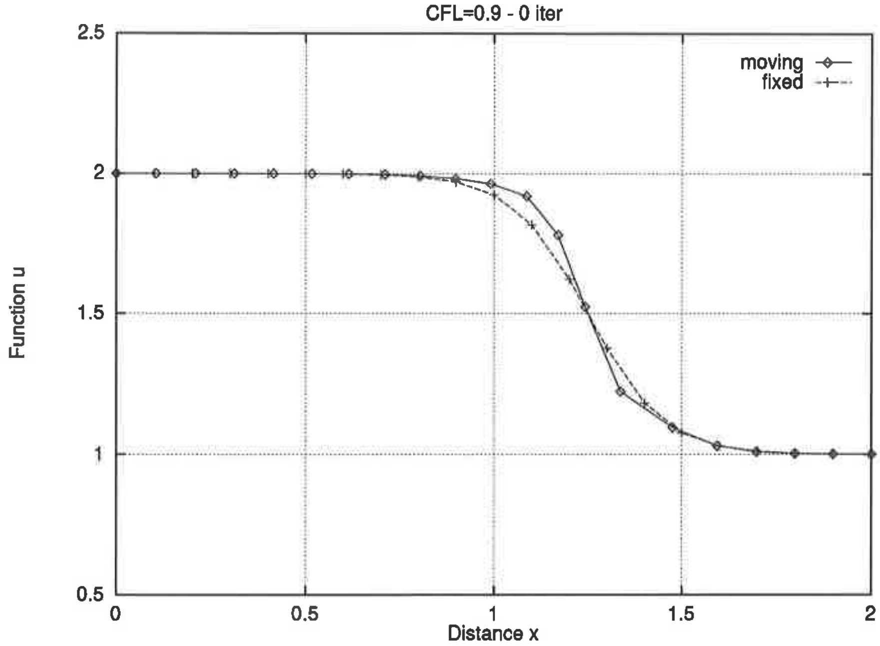

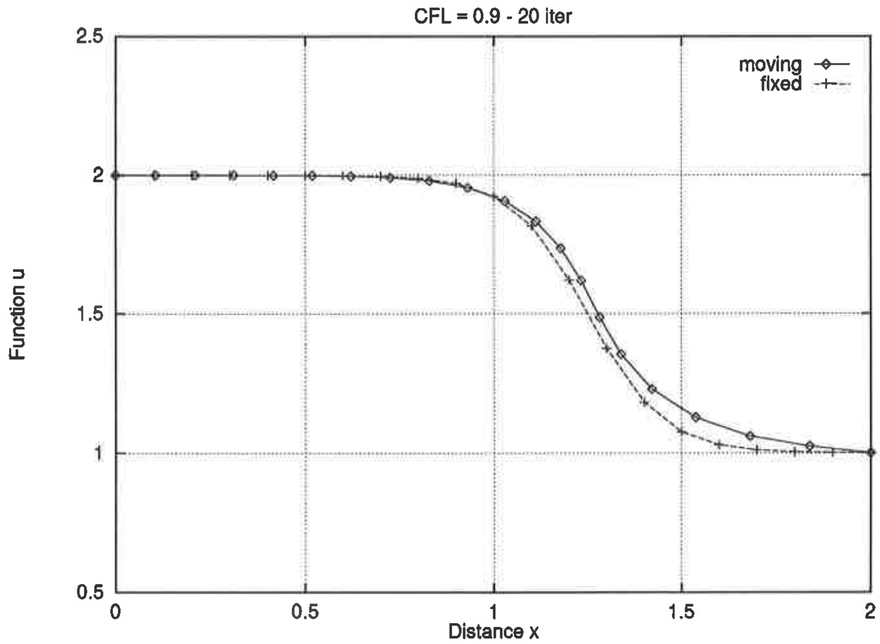

Figure 21: Equal arc length distribution. Linear advection. $\alpha = 5$. Upper: No iterations. Lower: 20 iterations

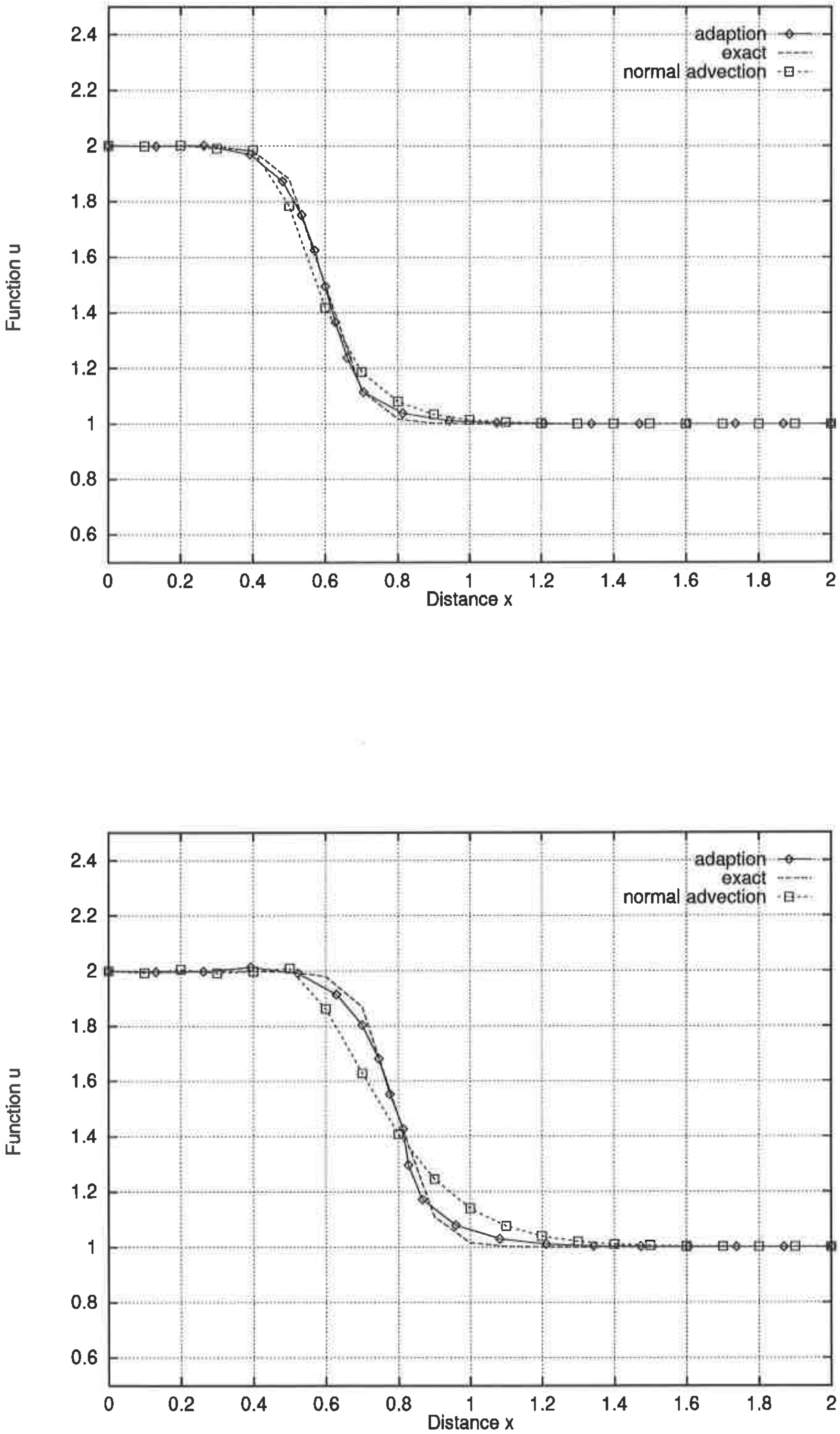

Figure 22: Equal arc length distribution. Linear advection. Implicit scheme. Upper: 1 time step. Lower: 10 time steps

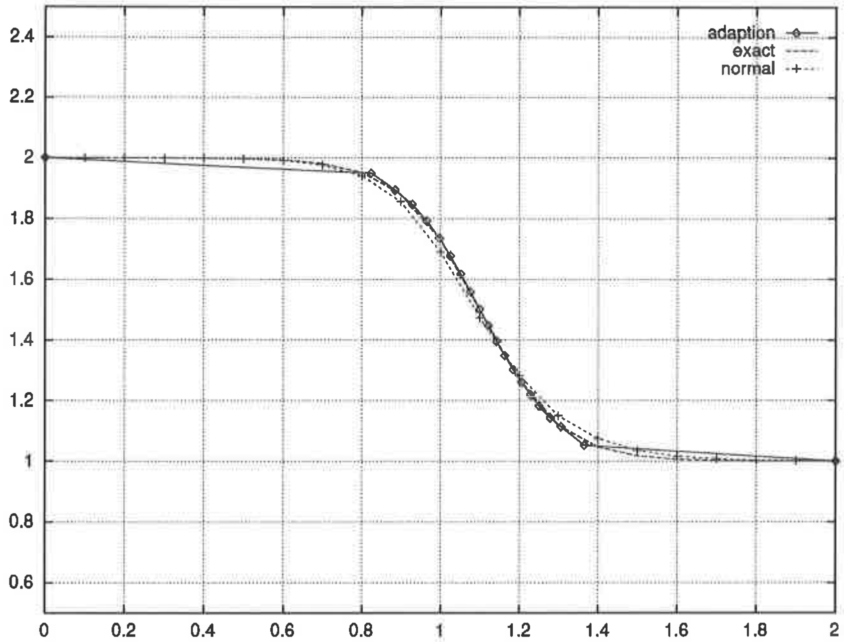

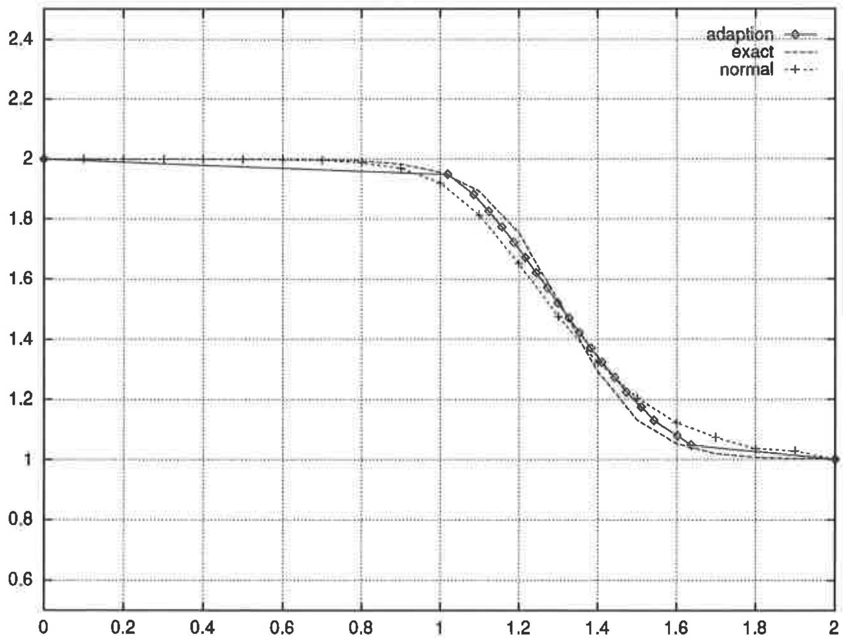

Figure 23: Equal 1st derivative distribution. Linear advection. Implicit scheme. Upper: 1 time step. Lower: 10 time steps

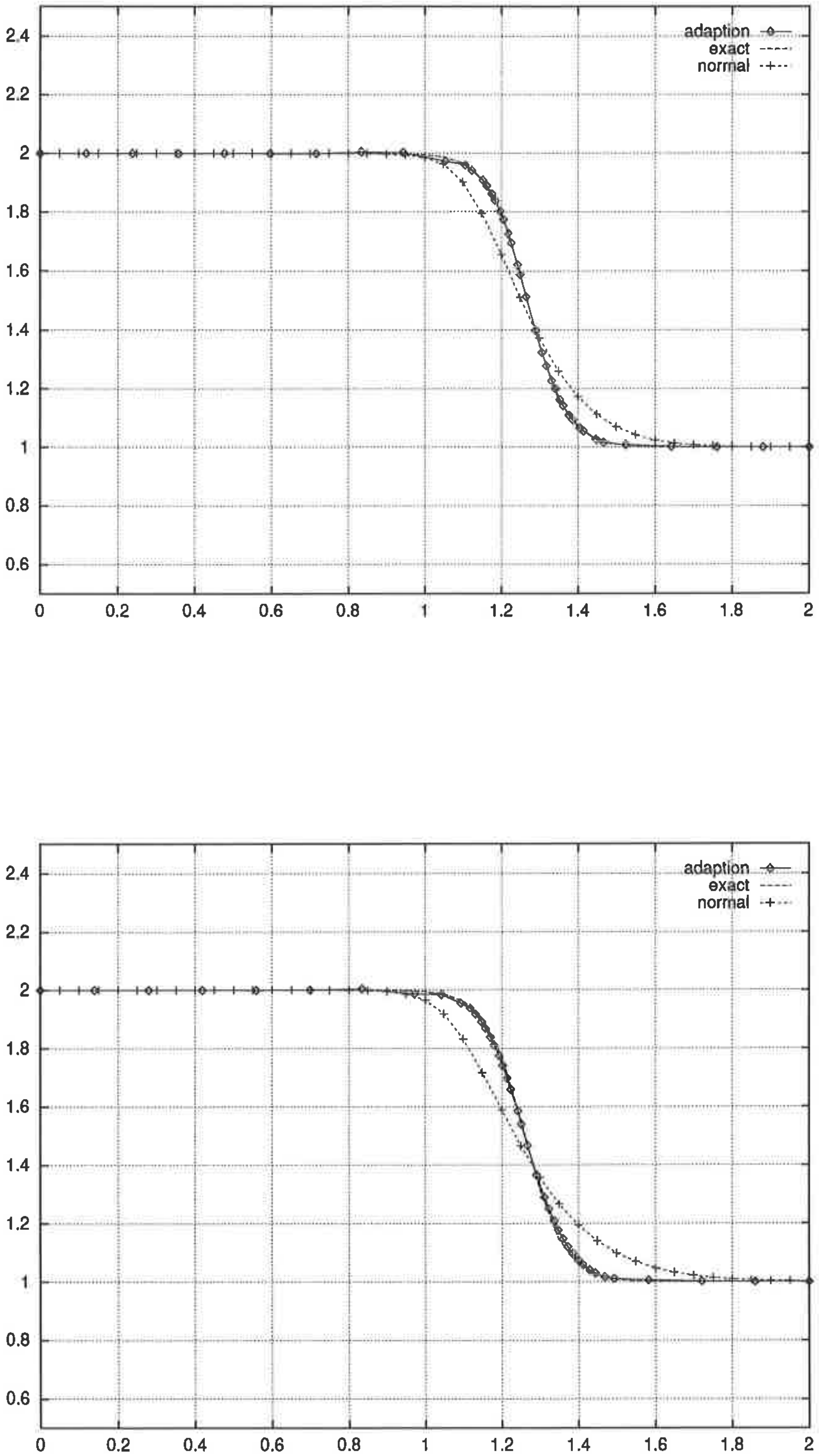

Figure 24: Equal 2nd derivative distribution. Linear advection. Implicit scheme with first approach. Upper: 30 time steps, cfl=1. Lower: 15 time steps cfl=2.

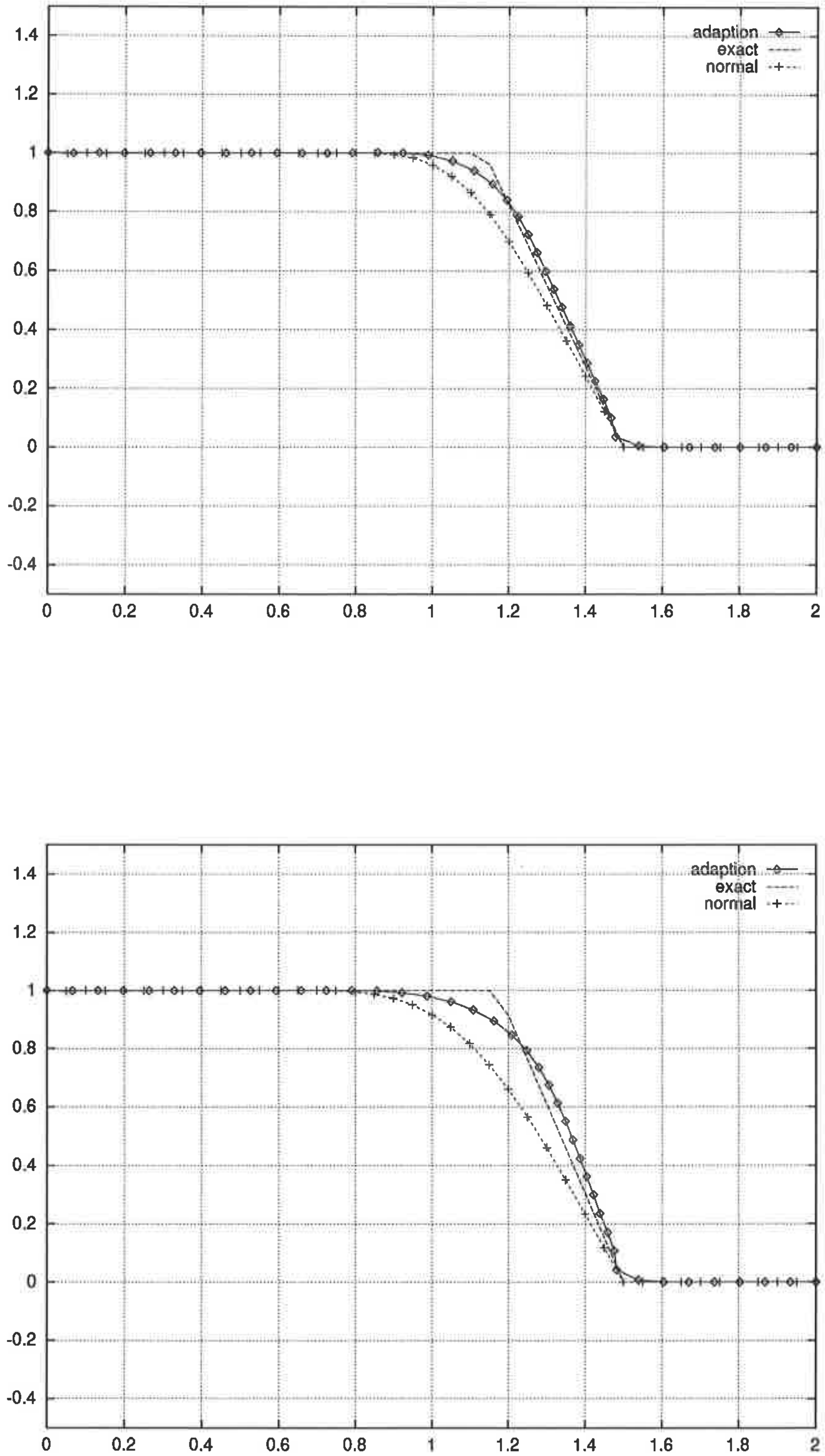

Figure 25: Equal arc length distribution. Non linear problem. Implicit scheme. Upper: Cfl=1. Lower: Cfl=2